Organic Electronics 13 (2012) 2104–2108

Contents lists available at SciVerse ScienceDirect

Organic Electronics

journal homepage: www.elsevier.com/locate/orgel

Upconversion effects on the performance of near-infrared laser-driven polymer photovoltaic devices

Jyh-Lih Wu [a], Fang-Chung Chen [a,*], Shu-Hao Chang [b], Kim-Shih Tan [a], Hsing-Yu Tuan [b]

[a] Department of Photonic and Display Institute, National Chiao Tung University, Hsinchu 30010, Taiwan
[b] Department of Chemical Engineering, National Tsing Hua University, Hsinchu 30013, Taiwan

ARTICLE INFO

Article history:
Received 8 May 2012
Received in revised form 28 May 2012
Accepted 29 May 2012
Available online 28 June 2012

Keywords:
Polymer
Upconversion
Photovoltaic
Laser

ABSTRACT

We have explored the upconversion (UC) effects resulting from the presence of $NaYF_4$:Yb/Er nanocrystals in near-infrared laser-driven organic photovoltaic devices (OPVs). Illumination of these UC nanomaterials with monochromatic light (980 nm) led to emission of visible light, which was subsequently absorbed by the polymer photoactive layer. We infer that both the long-wavelength charge-transfer absorption of the polymer blend and the UC effect contributed to the obvious near-infrared photovoltaic response. The resulting UC effects led to noticeable enhancements in the photocurrent and the efficiencies of the OPV devices under illumination at 980 nm.

1. Introduction

Organic photovoltaic devices (OPVs) feature several attractive properties, including light weight, semi-transparency, mechanical flexibility, and fabrication at low cost and low temperature [1–5]. Because the energy payback time (i.e., the time required for any energy-producing system or device to produce as much energy as was required in its manufacture) of flexible OPVs is potentially as short as several weeks [5], they are promising candidates for use in next-generation solar energy sources. Recently, we demonstrated a potential application of OPVs as wireless electrical sources that power biologically functionalized nanodevices when driven by near-infrared (NIR) lasers [6]. Because of the high transparency of biological tissues toward NIR photons, OPVs featuring a high photovoltaic response in the NIR spectral region could provide electrical power for biomedical sensing or diagnosis [6,7]. The NIR photovoltaic responses of such near-infrared laser-driven (NIRLD) polymer photovoltaic devices prepared from blends of poly(3-hexylthiophene) (P3HT) and [6,6]-phenyl-C_{61}-butyric acid methyl ester (PCBM) was resulted from their long-wavelength absorption of charge-transfer (CT) states [6]. Further efforts will be needed to improve the device efficiency toward NIR photons to meet the power requirements of future biological applications. In addition, the quantum efficiencies of most current OPVs in the NIR region remain very low. Because of the excitonic nature of the photogenerated species in organic semiconductors, the OPV active layer must feature both electron donor and acceptor components to overcome the strong exciton binding energy (e.g., typically 0.3–0.5 eV) at electron donor–acceptor (D–A) interfaces [3,8]. The need for energetic offset at the D–A interfaces limits the applicability of low-bandgap organic materials [8]. Therefore, taking advantage of the long-wavelength region of the solar spectrum is one potential means of further increasing the efficiencies of OPVs [8,9].

One feasible approach toward harvesting NIR photons is to exploit upconversion (UC) effects—that is, converting NIR radiation into visible photons [10–13]. Among established UC media, hexagonal $NaYF_4$ codoped with Yb^{3+} and Er^{3+} ions is one of the most promising materials [11,14]. In such a system, efficient UC can be achieved by

* Corresponding author. Tel.: +886 3 5131484; fax: +886 3 5735601.
E-mail address: fcchen@mail.nctu.edu.tw (F.-C. Chen).

1566-1199/$ - see front matter © 2012 Elsevier B.V. All rights reserved.
http://dx.doi.org/10.1016/j.orgel.2012.05.057

harvesting NIR photons with Yb^{3+} and emitting visible luminescence with Er^{3+}—i.e., through energy transfer from Yb^{3+} to Er^{3+} ions—followed by cross relaxation between two nearby Er^{3+} ions. The optical properties of these $NaYF_4$:Yb/Er nanocrystals (NCs) can be manipulated through tuning their sizes, shapes, and phases [10,14]. UC effects have been used previously to enhance the device efficiencies of silicon-based [15] and dye-sensitized [16] solar cells. Although preliminary results of the successful use of UC materials in organic solar cells have also been briefly reported [17], complete device characterization has not. In this study, we aimed to enhance the performance of NIRLD polymer photovoltaic devices, based on a blend of P3HT and PCBM, through the introduction of $NaYF_4$:Yb/Er NCs. Illumination of these UC phosphors with monochromatic light (980 nm) led to emission of visible light, which was subsequently absorbed by the polymer photoactive layer. In addition, to investigate the UC effects without influencing the electrical properties of the devices, we sprayed the $NaYF_4$:Yb/Er phosphors onto the back side of the completed device, rather than incorporating the material into the devices. This simple method boosted the conversion efficiency of the NIRLD polymer photovoltaic devices.

2. Experimental

Monodisperse hexagonal-phase $NaYF_4$:Yb/Er nanocrystals were prepared following the method as described by Chen et al. [18]. The NCs were synthesized through decomposition of NaF and lanthanide oleate complex in the presence of oleic acid and octadecene (as bifunctional linkers to control the shape and size of the NCs) at 320 °C. The resulting particle size, determined using transmission electron microscopy (TEM), was 40–50 nm (Fig. 1(a)). The steady-state photoluminescent (PL) spectrum was obtained using a continuous-wave laser at 980 nm as the excitation source. The devices were fabricated on ITO-coated glass substrates [6]. After a routine cleaning process, the glass substrates were dried in an oven for at least 12 h and then treated with UV ozone prior to use. The anodic buffer, poly(3,4-ethylenedioxythiophene):polystyrenesulfonate (PEDOT:PSS), was spin-coated on top of the indium tin

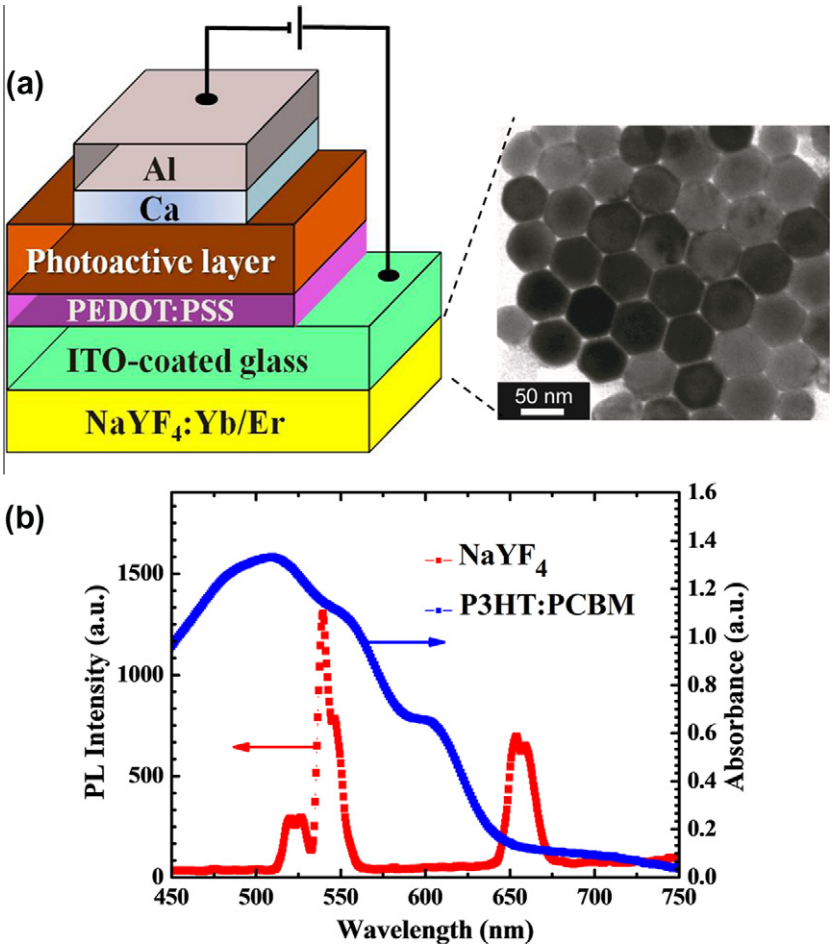

Fig. 1. (a) The left figure shows the schematic representation of the structure of the OPV incorporating $NaYF_4$:Yb/Er phosphors. The right figure displays the TEM image of the $NaYF_4$:Yb/Er NCs used in this study. (b) Absorption spectrum of a P3HT:PCBM (1:1, w/w) film and PL spectrum of the $NaYF_4$:Yb/Er NCs, recorded under excitation at 980 nm.

oxide (ITO)-coated substrates and then the samples were baked at 120 °C for 1 h. The photoactive layer, a solution of P3HT (Rieke Metals) and PCBM (Solenne) in 1,2-dichlorobenzene, was deposited on top of PEDOT:PSS. The thickness of the active layer was approximately 600 nm—thicker than those of most conventional devices to allow efficient NIR absorption. After undergoing solvent-annealing [19], the film was thermally annealed at 110 °C for 15 min in a N_2-filled glove box. To complete the device, a bilayer cathode comprising Ca (30 nm) and Al (100 nm) was deposited sequentially through thermal evaporation. The completed devices were encapsulated with a cover glass. The *I–V* characteristics of the OPVs were measured using a Keithley 2400 source measure unit. The photocurrent response was measured under illumination either from a 150-W Thermal Oriel solar simulator (AM 1.5G) or a 980-nm laser. The irradiation area of the 980-nm laser (ca. 3 mm^2) was smaller than the device area (10 mm^2). The absorption spectrum was recorded using a UV–vis–NIR spectrometer (PerkinElmer Lambda 950).

3. Results and discussion

To exploit UC effects, we sprayed a thick layer of $NaYF_4$:Yb/Er NCs from a hexane solution onto the back side of the glass substrate (Fig. 1(a)). We observed UC visible luminescence when we excited the NCs at 980 nm (Fig. 1(b)). The emission peaks (green and red) corresponded to different energy transfer processes [10,11]. Fig. 1(b) also displays the absorption spectrum of the P3HT:PCBM blend; the UC emission, especially the green one near 550 nm, overlapped well with the absorption spectrum of the active layer, suggesting efficient absorption in this UC OPV system.

Fig. 2(a) displays a cross-sectional SEM image of the UC film obtained after spray-coating; the average film thickness was approximately 5 μm. The top-view image of the film (Fig. 2(b)) suggests that the film surface was quite rough. The cotton-like morphology of the UC material probably resulted from the high volatility of the solvent (hexane) used for spray-coating. Together with the high pressure of the carrier gas (N_2), the UC NCs solidified quickly, resulting in a rough surface. Nevertheless, although the surface of the UC film was rough, we could still observe an apparent UC process. Considering that this approach is compatible with the fabrication of large-area devices, our results suggest that a simple spray-coating process might be a promising means of preparing practically useful UC thin films.

Fig. 3(a) illustrates the effect of the UC on the devices' current–voltage (*I–V*) characteristics, recorded under illumination from a 980-nm laser at a power of 146 mW.

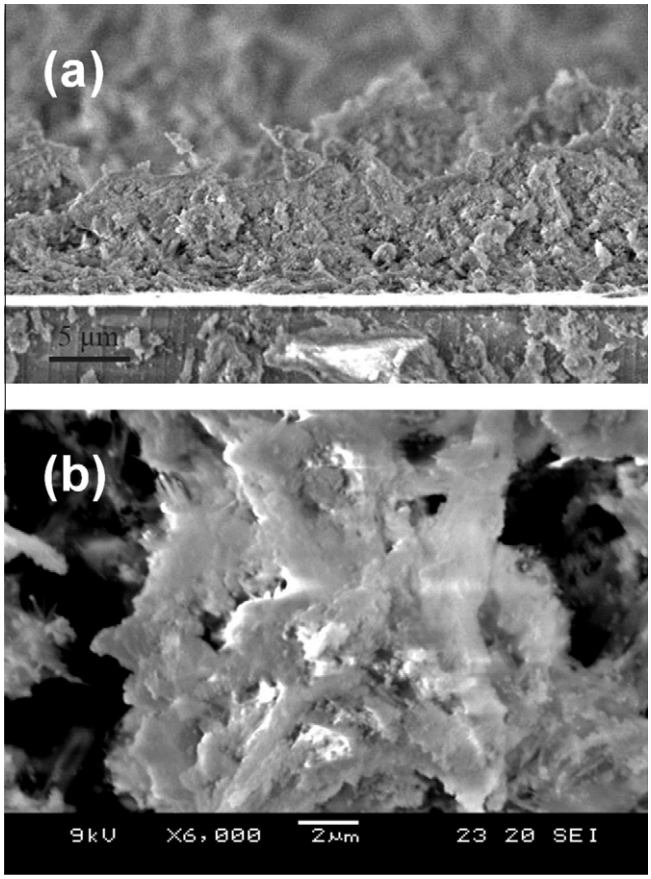

Fig. 2. (a) Cross-sectional and (b) top-view SEM images of a $NaYF_4$:Yb/Er thin film prepared using the spray-coating approach.

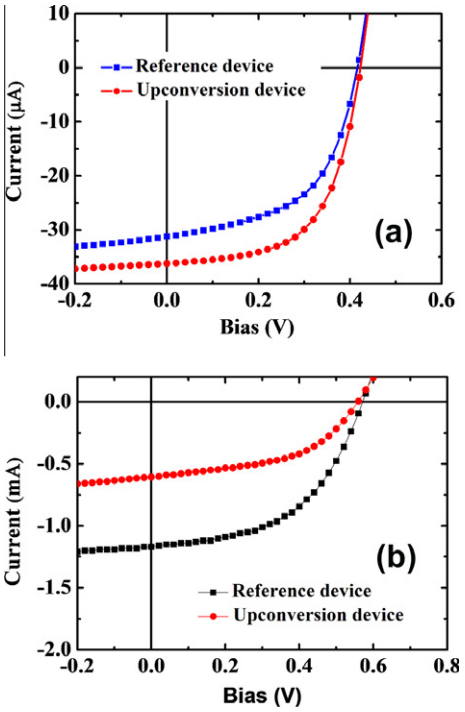

Fig. 3. *I–V* characteristics of OPV devices, recorded under illumination with (a) a 980-nm laser at a power of 146 mW and (b) simulated solar light (AM 1.5G) at 100 mW cm^{-2}.

The reference device possessing the structure ITO/PEDOT:PSS/P3HT:PCBM/Ca/Al exhibited an open-circuit voltage (V_{oc}) of 0.41 V, a short-circuit current (I_{sc}) of 31.2 μA, and a fill factor (FF) of 0.55, yielding a power conversion efficiency (PCE) of 0.0048%. These values are comparable with those of previously reported devices [6]. After applying the UC NCs, the values of V_{oc} and FF increased slightly, to 0.43 V and 0.58, respectively; more importantly, the value of I_{sc} increased to 36.2 μA, enhancing the PCE to 0.0062%. Meanwhile, the maximum output power, defined as the product of the maximum photocurrent multiplied by the maximum voltage, was enhanced by approximately 30% (from 7.00 to 9.05 μW). When we characterized our device under illumination with simulated solar irradiation (AM 1.5G), however, the UC effects did not improve the device efficiency. Fig. 3(b) reveals that the photocurrent of the reference device decreased significantly when using the UC NCs. We suspect that a huge portion of the incoming photons was scattered or blocked by the $NaYF_4$:Yb/Er thin film, leading to decreased device performance. Furthermore, because efficient UC occurs only at high levels of light intensity, we expected very minor UC effects to exist in our device system under normal solar illumination conditions.

The NIR photovoltaic response of the device resulted from two major effects. First, the 980-nm photons could directly excite the CT states present in the polymer/fullerene blends, leading to a pronounced photocurrent [6,20,21]. Second, as revealed in Fig. 1(b), the UC visible

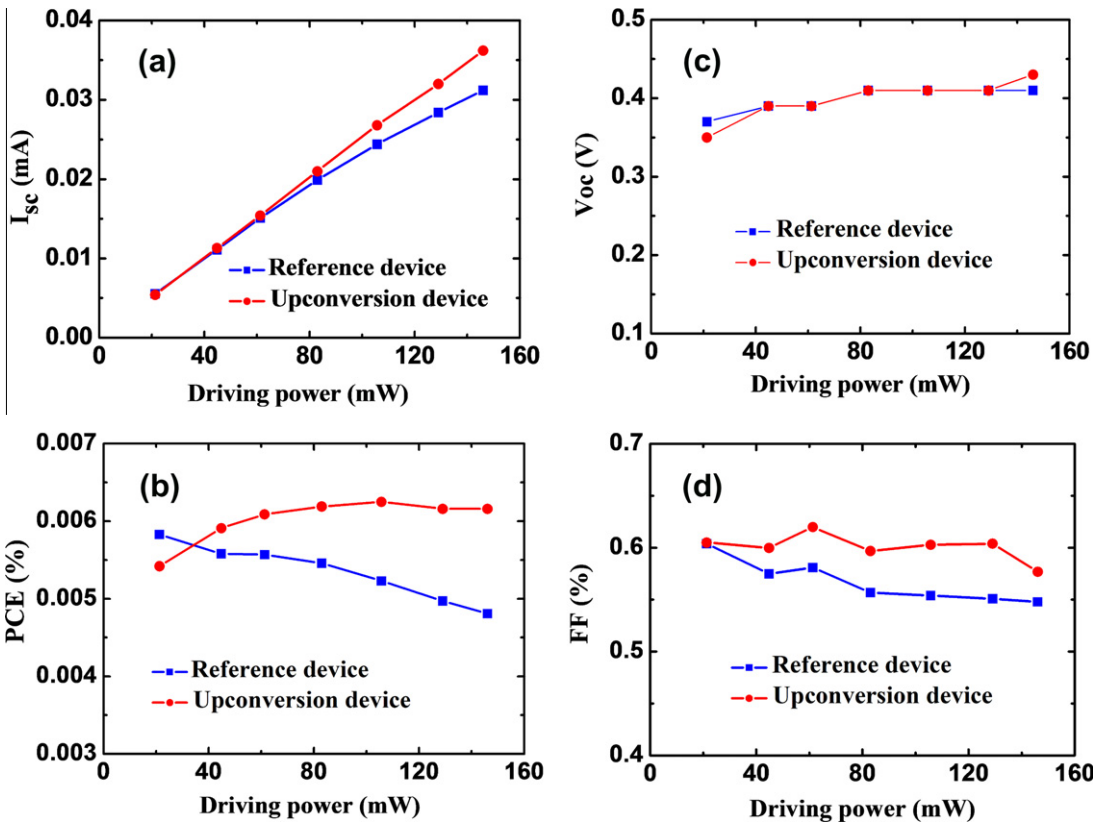

Fig. 4. Values of (a) I_{sc}, (b) PCE, (c) V_{oc}, and (d) FF of NIRLD OPVs, prepared with and without UC NCs, plotted with respect to the power of a 980-nm laser.

luminescence could be absorbed by the P3HT:PCBM thin film, resulting in another possible route for charge carrier generation. Therefore, we infer that the additional photocurrent contributed by the UC process improved the device performance.

Next, we studied the effect of the irradiation power on the photovoltaic characteristics of the NIRLD devices to obtain further insight into the mechanism responsible for the enhanced device performance. Fig. 4(a) reveals that the photocurrent of the reference device deviated from a linear dependence at higher laser powers. In a previous report, we attributed such deviation to possible photodegradation of the photoactive layer under high-intensity illumination [6]. The photocurrent of the UC device, however, scaled linearly with the illumination intensity—even at high intensity. This behavior might be due to the $NaYF_4$:Yb/Er NCs on the front of the device absorbing a large number of the NIR photons, thereby minimizing any possible photodegradation under high-intensity illumination. Furthermore, the incorporation of the UC materials also modified the effect of the irradiation power on the PCEs (Fig. 4(b)). The decreased FFs and the deviation of the photocurrent from linear dependence resulted in the PCEs decreasing upon increasing the laser power. In addition, at lower levels of laser power (ca. <30 mW), the presence of these UC NCs in the NIRLD devices did not improve the PCE (Fig. 4(b)). This observation is not surprising because multiple photons are involved in the UC process [22]. Because a high laser power was required to obtain efficient UC luminescence, the PCEs for the UC device increased upon increasing the power of the 980-nm laser. The distinct trends in the dependence of the irradiation power further account for the presence of the UC effects.

4. Conclusion

The presence of UC $NaYF_4$:Yb/Er NCs improves the device performance of NIRLD OPVs, with both the long-wavelength CT absorption and the UC contributing to the obvious NIR photon response. We observed entirely different effects of the laser power on the photovoltaic characteristics of the devices prepared with and without the UC NCs. The UC effects led to noticeable enhancements in the photocurrents and efficiencies of the OPV devices under illumination with monochromatic light at 980 nm, suggesting that UC nanomaterials have great potential for application in OPVs.

Acknowledgements

We thank the National Science Council of Taiwan (NSC 100-2221-E-009-082, NSC 100-2628-E-007-029-MY2 and NSC 101-3113-E-009-005) and the Ministry of Education of Taiwan (through the ATU program) for financial support.

References

[1] C.J. Brabec, N.S. Sariciftci, J.C. Hummelen, Adv. Funct. Mater. 11 (2001) 15.
[2] G. Li, V. Shrotriya, J.S. Huang, Y. Yao, T. Moriarty, K. Emery, Y. Yang, Nat. Mater. 4 (2005) 864.
[3] J.D. Servaites, M.A. Ratner, T.J. Marks, Energy Environ. Sci. 4 (2011) 4410.
[4] S.H. Park, A. Roy, S. Beaupre, S. Cho, N. Coates, J.S. Moon, D. Moses, M. Leclerc, K. Lee, A.J. Heeger, Nat. Photonics 3 (2009) 297.
[5] A.L. Roes, E.A. Alsema, K. Blok, M.K. Patel, Prog. Photovoltaics Res. Appl. 17 (2009) 372.
[6] J.L. Wu, F.C. Chen, M.K. Chuang, K.S. Tan, Energy Environ. Sci. 4 (2011) 3374.
[7] Z.G. Chen, L.S. Zhang, Y.G. Sun, J.Q. Hu, D.Y. Wang, Adv. Funct. Mater. 19 (2009) 3815.
[8] G. Dennler, M.C. Scharber, C.J. Brabec, Adv. Mater. 13 (2009) 1338.
[9] M.C. Scharber, D. Mühlbacher, M. Koppe, P. Denk, C. Waldauf, A.J. Heeger, C.J. Brabec, Adv. Mater. 18 (2006) 789.
[10] H.X. Mai, Y.W. Zhang, L.D. Sun, C.H. Yan, J. Phys. Chem. C 111 (2007) 13721.
[11] S. Schietinger, L. de S. Menezes, B. Lauritzen, O. Benson, Nano Lett. 9 (2009) 2477.
[12] S. Heer, K. Kömpe, H.U. Güdel, M. Haase, Adv. Mater. 16 (2004) 2102.
[13] H.Q. Wang, T. Nann, ACS Nano 3 (2009) 3804.
[14] L. Wang, Y. Li, Chem. Mater. 19 (2007) 727.
[15] A. Shalav, B.S. Richards, T. Trupke, K.W. Krämer, H.U. Güdel, Appl. Phys. Lett. 86 (2005) 013505.
[16] G.B. Shan, G.P. Demopoulos, Adv. Mater. 22 (2010) 4373.
[17] H.Q. Wang, M. Batentschuk, A. Osvet, L. Pinna, C.J. Brabec, Adv. Mater. 2 (2011) 2675.
[18] C. Liu, H. Wang, X. Li, D. Chen, J. Mater. Chem. 19 (2009) 3546.
[19] G. Li, Y. Yao, H. Yang, V. Shrotriya, G. Yang, Y. Yang, Adv. Funct. Mater. 17 (2007) 1636.
[20] K. Vandewal, K. Tvingstedt, A. Gadisa, O. Inganäs, J.V. Manca, Nat. Mater. 8 (2009) 904.
[21] K. Vandewal, A. Gadisa, W.D. Oosterbaan, S. Bertho, F. Banishoeib, I.V. Severen, L. Lutsen, T.J. Cleij, D. Vanderzande, J.V. Manca, Adv. Funct. Mater. 18 (2008) 2064.
[22] B. Ahrens, P. Löper, J.C. Goldschmidt, S. Glunz, B. Henke, P.T. Miclea, S. Schweizer, Phys. Status Solidi A 205 (2008) 2822.